PLOS ONE

RESEARCH ARTICLE

# Flattening Filter-Free Beams in Intensity-Modulated Radiotherapy and Volumetric Modulated Arc Therapy for Sinonasal Cancer

**Jia-Yang Lu[1☯], Jing Zheng[2☯], Wu-Zhe Zhang[1☯], Bao-Tian Huang[1]***

**1** Department of Radiation Oncology, Cancer Hospital of Shantou University Medical College, Shantou, Guangdong, China, **2** Department of Laboratory, Shantou Central Hospital, Affiliated Shantou Hospital of Sun Yat-sen University, Shantou, Guangdong, China

☯ These authors contributed equally to this work.
* tianjia2025@163.com





**Citation:** Lu J-Y, Zheng J, Zhang W-Z, Huang B-T (2016) Flattening Filter-Free Beams in Intensity-Modulated Radiotherapy and Volumetric Modulated Arc Therapy for Sinonasal Cancer. PLoS ONE 11(1): e0146604. doi:10.1371/journal.pone.0146604

**Editor:** Shian-Ying Sung, Taipei Medical University, TAIWAN

**Received:** October 5, 2015

**Accepted:** December 18, 2015

**Published:** January 6, 2016



**Data Availability Statement:** All relevant data are within the paper.

**Funding:** This work was supported by Shantou Medical Science and Technology Project [Grant No. (2015)123] and Medical Scientific Research Foundation of Guangdong Province (Grant No. A2015534). No additional external funding was received for this study. The funders had no role in study design, data collection and analysis, decision to publish, or preparation of the manuscript.

**Competing Interests:** The authors have declared that no competing interests exist.

## Abstract

### Purpose

To evaluate the dosimetric impacts of flattening filter-free (FFF) beams in intensity-modulated radiotherapy (IMRT) and volumetric modulated arc therapy (VMAT) for sinonasal cancer.

### Methods

For fourteen cases, IMRT and VMAT planning was performed using 6-MV photon beams with both conventional flattened and FFF modes. The four types of plans were compared in terms of target dose homogeneity and conformity, organ-at-risk (OAR) sparing, number of monitor units (MUs) per fraction, treatment time and pure beam-on time.

### Results

FFF beams led to comparable target dose homogeneity, conformity, increased number of MUs and lower doses to the spinal cord, brainstem and normal tissue, compared with flattened beams in both IMRT and VMAT. FFF beams in IMRT resulted in improvements by up to 5.4% for sparing of the contralateral optic structures, with shortened treatment time by 9.5%. However, FFF beams provided comparable overall OAR sparing and treatment time in VMAT. With FFF mode, VMAT yielded inferior homogeneity and superior conformity compared with IMRT, with comparable overall OAR sparing and significantly shorter treatment time.

### Conclusions

Using FFF beams in IMRT and VMAT is feasible for the treatment of sinonasal cancer. Our results suggest that the delivery mode of FFF beams may play an encouraging role with better sparing of contralateral optic OARs and treatment efficiency in IMRT, but yield comparable results in VMAT.

## Introduction

Sinonasal cancers (SNCs) are uncommon, accounting for only 3–5% of all head and neck malignancies [1–3]. They are typically diagnosed at locally advanced stages, where surgical operation and postoperative radiation therapy represent the standard of care [4,5]. Over the last decade, intensity-modulated radiotherapy (IMRT) and volumetric modulated arc therapy (VMAT) have become prevalent treatment techniques for SNCs [6–8], owing to their dosimetric advantages along with the clinical preservation of nearby optic structures [9–11] while maintaining disease control and survival. However, treatment planning for SNC is challenging due to the proximity and/or involvement of multiple critical organs at risk (OARs) including the optic nerves, optic chiasm, lenses, brain, parotid glands and brainstem. Making compromises is sometimes necessary in order to avoid overdosing the optic structures [12] or ensure target dose coverage. How to design radiotherapy plans for SNC remains an interesting investigative topic.

Conventional radiation beams from medical linear accelerators are flattened in order to generate a homogeneous dose distribution at a certain depth for an open treatment field, by inserting a flattening filter into the head of the linear accelerators. In recent years, there has been a growing interest in the removal of the flattening filter, which results in a flattening filter-free (FFF) beam. The FFF beams are characterized by high dose rate, cone-like fluence profile, softened beam quality [13], increased superficial dose, reduced out-of-field dose [14,15] and high dose calculation accuracy (at least as high as for flattened beams) [16]. Modern radiotherapy techniques, such as IMRT and VMAT, are able to generate intensity modulated beams using multi-leaf collimator (MLC) motion series in combination with inverse planning. Since the fluence profile can be taken into consideration during optimization, the conventional flattened beams become unnecessary in this situation. The clinical application of FFF beams has been investigated in many studies for the cases of breast cancer [17], lung cancer [18] and other tumor sites [19–23]. These studies concluded in general that the FFF beams resulted in similar plan qualities and reduction of treatment time. However, none of these studies has been focused on dosimetric roles of FFF beams in the SNC cases. As the FFF beams can deliver lower out-of-field dose, there might be some potential dosimetric benefits with respect to the sparing of lenses or other OARs. Therefore, we compared the FFF beams with conventional beams in the IMRT and VMAT for SNC in this study, aiming to identify the dosimetric effects of this delivery mode and selecting the reasonable radiotherapy technique for the treatment of SNC.

## Methods

### Ethics statement

The protocol was approved by the Ethical Commission of the Cancer Hospital of Shantou University Medical College. Because this was not a treatment-based study, our institutional review board waived the need for written informed consent from the participants. The patient information was anonymized and de-identified to protect patient confidentiality.

### Patient characteristics

Computed tomography (CT) scan datasets of 14 patients diagnosed as melanoma (Patients 1–3), esthesioneuroblastoma (Patients 4 and 5), squamous cell carcinoma (Patients 6–9), adenoid cystic carcinoma (Patient 10), sarcoma (Patient 11) and NK/T cell lymphoma (Patients 12–14) of the nasal cavity, maxillary sinus and ethmoid sinus were selected. The patients included 8 males and 6 females, with a median age of 62 years (range, 32–66 years). In

accordance with the American Joint Committee on Cancer (AJCC) Seventh Edition staging system, the patients were at stage T2-T4, N0 and M0. All the patients received surgical operations followed by postoperative radiotherapy except for the 3 NK/T cell lymphoma patients who received radiotherapy alone.

## CT simulation and the delineation of target and OARs

All the patients were immobilized in supine position in a tailor-made head-neck-shoulder thermoplastic cast. CT scans with a 3-mm slice thickness were performed using a 16-slice CT scanner (Philips Brilliance CT Big Bore Oncology Configuration, Cleveland, OH, USA). The CT images were then transferred to the Eclipse$^{TM}$ version 10.0 treatment planning system (Varian Medical System, Inc., Palo Alto, CA) for target and OAR delineation and treatment planning.

All target volumes were delineated by our radiation oncologists. Gross tumor volume (GTV) was defined as the visible extent of tumor identified utilizing contrasted CT, MR and positron emission tomography (PET) for definitively treated patients. The clinical target volume (CTV) comprises the primary tumor bed and the zones at risk of harboring microscopic extension. The planning target volume (PTV) was derived from the clinical target volume plus a uniform 5-mm margin, and was then cropped 3 mm away from the surface of the body to avoid the parts extending outside the body and the build-up effect. The median volume of the PTV was 185 cubic centimeters (cc) with a range of 102–259 cc.

The OARs included the lenses, optic nerves, optic chiasm, eyes, spinal cord, brainstem, temporal lobes, cochleae, pituitary, oral cavity and parotids. The "PTV_in_skin" was generated from the portion of PTV within a ring structure generated by a 7-mm inner margin of the body [20]. Surrounding normal tissue was defined as the body volume excluding the PTV.

## Linear accelerator calibration

A TrueBeam® (Varian Medical System, Inc., Palo Alto, CA) linear accelerator was used to deliver 6-MV FFF beams and conventional flattened beams. The output of both beams were calibrated such that 1 MU gave 0.01-Gy dose to water at central axis at a depth of maximum dose for a field size of $10 \times 10$ cm$^2$ and for a source-to-surface distance (SSD) of 100 cm.

## Radiotherapy treatment planning

The IMRT plans using non-coplanar 6-MV FFF beams (FFF-IMRT) and conventional flattened beams (C-IMRT) from TrueBeam® were generated in Eclipse$^{TM}$. The beam arrangement was set according to the study by Jeong *et al* [4] with minor modifications (Field 1/Field 2, gantry 260°/100° with collimator 330°/30° and couch 0°; Field 3/Field 4, gantry 330°/30° with collimator angles optimized to minimize the exposure to the lenses, with fixed jaw and with couch 0°; Field 5, gantry 0° with collimator 0° and couch 0°; Field 6/Field 7, gantry 330°/30° with collimator 0° and couch 90°). The VMAT plans with 6-MV FFF beams (FFF-VMAT) or conventional flattened beams (C-VMAT) were generated using two coplanar arcs of 360° with collimators rotated to 30° and 330°, respectively to minimize the tongue and groove effect. Maximum dose rates of 600 and 1400 monitor units (MUs)/minute were selected for the conventional flattened and FFF beams, respectively. Prescription doses were set to 60 Gy (2 Gy/fraction) administered in 30 fractions for both IMRT and VMAT. Optimizations were performed with the Dose Volume Optimizer (DVO, version 10.0.28) and Progressive Resolution Optimizer (PRO, version 10.0.28) algorithms for IMRT and VMAT, respectively. The Anisotropic Analytical Algorithm (AAA, version 10.0.28) was applied for final dose calculations, with a grid size of 2.5 mm. Dose-limiting ring structures were generated to form the dose

gradients surrounding the PTV. Each treatment plan was normalized such that 95% of the PTV received the prescribed dose of 60 Gy.

The same optimization objectives were adopted for the FFF-IMRT, C-IMRT, FFF-VMAT and C-VMAT plans. The IMRT plans were further optimized utilizing Eclipse$^{TM}$'s "base dose plan" function to improve the plan qualities. The "base dose plan" function enabled the system to optimize a plan (as a second plan) while taking another plan (as a base dose plan) into account, aiming to achieve an optimal plan sum by making up for inadequacies (hot/cold spots) in the base dose plan. Our approach utilizing the "base dose plan" function is described briefly as follows: with optimization objectives being unmodified, the treatment plan duplicated from the original plan with half of total fractions was further optimized based on the original plan with half of total fractions, and then the number of fractions of the treatment plan was restored from a half to the total. The details of this approach applied in head-and-neck cancer were introduced in our previous study [24]. The VMAT plans were further optimized once or twice to improve the plan qualities. Treatment planning goals are listed in Table 1. $D_{x\%}$ represents the dose which is reached or exceeded in x% of the volume and $V_{xGy}$ represents the % volume receiving a dose of x Gy. $D_{2\%}$ and $D_{98\%}$ represent the near-maximum and near-minimum doses, respectively according to the International Commission on Radiation Units and Measurements (ICRU) report 83 [25]. $D_{mean}$ represents the mean dose. The optimization objectives were adjusted to ensure that the $D_{2\%}$ of PTV was below the 110% of the prescription dose. The sparing of lenses, optic chiasm and optic nerves was set to the highest priority with the aim of preserving at least unilateral vision, followed by the PTV coverage objectives. The sparing of brainstem and spinal cord was set to the third priority, and the dose limitations of the remaining OARs and ring structures were set to the last priority.

All the plans were conducted by one medical physicist to avoid individual variation. The numbers of MUs per fraction were compared. The treatment time which included the gantry and couch rotation time but excluded the patient setup time was recorded. Additionally, the pure beam-on time of the linear accelerator was also recorded. The treatment efficiency was

**Table 1. Treatment planning goals for sinonasal cancer.**

| Structure | Planning constraint(s) |
|---|---|
| **PTV** | $D_{95\%}$ = 60 Gy |
| | $D_{2\%}$ < 66 Gy (110% of the prescription dose) |
| **Lens** | $D_{2\%}$ < 10 Gy |
| **Optic nerve** | $D_{2\%}$ < 54 Gy |
| **Optic chiasm** | $D_{2\%}$ < 54 Gy |
| **Eye** | $D_{2\%}$ < 50 Gy |
| **Spinal cord** | $D_{2\%}$ < 40 Gy |
| **Brainstem** | $D_{2\%}$ < 50 Gy |
| **Temporal lobe** | $D_{2\%}$ < 60 Gy |
| **Cochlea** | $D_{5\%}$ < 55 Gy, $D_{mean}$ < 45 Gy |
| **Pituitary** | $D_{2\%}$ < 60 Gy |
| **Oral cavity** | $D_{mean}$ < 30 Gy |
| **Parotid** | $D_{50\%}$ < 30 Gy, $D_{mean}$ < 26 Gy |
| **Normal tissue** | As low as possible |

PTV = planning target volume; $D_{x\%}$ = dose that is reached or exceeded in x% of the volume; $D_{mean}$ = mean dose.

doi:10.1371/journal.pone.0146604.t001

defined as the treatment task completed by the linear accelerator per unit of treatment time. The treatment efficiency is inversely proportional to the treatment time [26].

### Plan evaluation

Dose-volume statistics, isodose distributions and cumulative dose-volume histograms (DVHs) were computed to compare the plans. $D_{2\%}$ and $D_{98\%}$ were selected for the appraisals of hot and cold spots, respectively. The target dose homogeneity was quantified using the homogeneity index (HI) recommended by the ICRU report 83 [25]. The target dose conformity was measured using the conformity index (CI) proposed by Paddick [27].

### Statistical analysis

To determine the statistical significance of the differences among the techniques, two-tailed paired Wilcoxon signed-rank tests were performed with a *P*-value of $< 0.05$ considered to be significant, using SPSS version 19 software (SPSS, Inc., Chicago, IL, USA).

## Results

### Target coverage, homogeneity and conformity

All the PTVs received sufficient dose coverage. For each plan, the $D_{95\%}$ of PTV was normalized to 60 Gy and the $D_{2\%}$ of the PTV was lower than 66 Gy. The data for the PTV (Table 2) demonstrate that the $D_{2\%}$ values, $D_{98\%}$ values, HIs and CIs were comparable between the FFF beams and conventional flattened beams both for IMRT and VMAT ($P > 0.05$), and the $D_{98\%}$ of PTV_in_skin was increased by 0.9% with FFF beams in IMRT. When compared to FFF-IMRT, FFF-VMAT yielded 1% higher $D_{2\%}$ and 0.7% lower $D_{98\%}$ for the PTV, and produced inferior HI by 29.7% and superior CI by 2.7%. In the isodose distribution, fewer hot spots of $\geq$ 105% (63 Gy) of the prescribed dose for the PTV were observed for IMRT (Fig 1).

### OAR sparing

The doses delivered to all the OARs, except the ipsilateral lens and optic nerve that were in close proximity to or a part of the PTV, were limited to the tolerance levels. As shown in Table 2, FFF-IMRT allowed additional $D_{2\%}$ reductions of 5.4%, 3.2%, 3.0% and 0.8% with regards to the contralateral lens, contralateral eye, spinal cord and brainstem, respectively compared with C-IMRT. FFF-IMRT also gave smaller $V_{5Gy}$, $V_{10Gy}$, $V_{20Gy}$ and $V_{30Gy}$ of normal tissue by 1.4%, 0.6%, 0.2% and 0.2%, respectively. When compared with C-VMAT, FFF-VMAT provided lower $D_{2\%}$ to the ipsilateral lens, optic chiasm, spinal cord and brainstem, by 1.7%, 2.2%, 9.8% and 5.5%, respectively, but delivered higher $D_{2\%}$ to the ipsilateral optic nerve, contralateral eye and ipsilateral eye by 1.0%, 5.8% and 2.2%, respectively. With respect to the normal tissue, minor improvements with FFF beams were observed in terms of $V_{5Gy}$, $V_{10Gy}$ and $V_{20Gy}$ by 0.7%, 1.3% and 0.4%, respectively, along with similar $V_{30Gy}$.

As to the comparison of FFF-IMRT and FFF-VMAT, FFF-IMRT tended to deposit lower doses to most of the optic structures including the contralateral lens and bilateral optic nerves by 3.9%-18.4%, and displayed better sparing of the contralateral cochlea and bilateral parotids. However, FFF-VMAT exhibited significant dose reduction of the spinal cord, brainstem, ipsilateral temporal lobe, pituitary and oral cavity by 8.3%-45.0%. Concerning the normal tissue, smaller $V_{5Gy}$ was identified for FFF-VMAT while smaller $V_{20Gy}$ and $V_{30Gy}$ were observed for FFF-IMRT ($P < 0.05$). These results are also illustrated in Fig 2 for Patient 4.

**Table 2. Dosimetric parameters for the flattening filter-free intensity-modulated radiotherapy (FFF-IMRT), conventional IMRT (C-IMRT), flattening filter-free volumetric modulated arc therapy (FFF-VMAT) plans and conventional VMAT (C-VMAT).**

| | | FFF-IMRT | C-IMRT | FFF-VMAT | C-VMAT | *P*-value | | |
|---|---|---|---|---|---|---|---|---|
| | | | | | | FFF-IMRT *vs* C-IMRT | FFF-VMAT *vs* C-VMAT | FFF-IMRT *vs* FFF-VMAT |
| **PTV** | **$D_{2\%}$ (Gy)** | 62.98 ± 0.69 | 62.90 ± 0.76 | 63.63 ± 0.98 | 63.53 ± 0.76 | 0.330 | 0.490 | 0.001 |
| | **$D_{98\%}$ (Gy)** | 59.40 ± 0.25 | 59.34 ± 0.25 | 58.96 ± 0.29 | 58.96 ± 0.29 | 0.064 | 0.878 | 0.001 |
| | **$D_{50\%}$ (Gy)** | 61.26 ± 0.27 | 61.26 ± 0.31 | 61.96 ± 0.68 | 61.88 ± 0.48 | 0.889 | 0.124 | 0.001 |
| | **HI** | 0.058 ± 0.014 | 0.058 ± 0.016 | 0.075 ± 0.019 | 0.074 ± 0.016 | 0.875 | 0.470 | 0.001 |
| | **CI** | 0.869 ± 0.019 | 0.865 ± 0.016 | 0.892 ± 0.020 | 0.896 ± 0.016 | 0.245 | 0.074 | 0.003 |
| **PTV_in_skin** | **$D_{98\%}$ (Gy)** | 56.48 ± 1.19 | 55.97 ± 1.39 | 56.64 ± 0.70 | 56.57 ±0.76 | 0.016 | 0.258 | 0.433 |
| **CL lens** | **$D_{2\%}$ (Gy)** | 6.50 ± 1.31 | 6.84 ± 1.21 | 7.95 ± 0.95 | 7.96 ± 0.85 | 0.002 | 0.778 | 0.001 |
| **IL lens** | **$D_{2\%}$ (Gy)** | 8.98 ± 2.15 | 9.10 ± 2.15 | 8.78 ± 1.59 | 8.92 ± 1.50 | 0.363 | 0.030 | 0.451 |
| **CL optic nerve** | **$D_{2\%}$ (Gy)** | 43.85 ± 9.69 | 44.48 ± 9.63 | 49.50 ± 4.86 | 49.41 ± 5.08 | 0.103 | 0.683 | 0.005 |
| **IL optic nerve** | **$D_{2\%}$ (Gy)** | 52.09 ± 4.06 | 52.16 ± 3.55 | 54.20 ± 3.26 | 53.70 ± 3.62 | 0.683 | 0.011 | 0.001 |
| **Optic chiasm** | **$D_{2\%}$ (Gy)** | 45.40 ± 6.95 | 45.82 ± 6.57 | 44.06 ± 10.42 | 44.81 ± 9.65 | 0.198 | 0.026 | 0.510 |
| **CL eye** | **$D_{2\%}$ (Gy)** | 33.62 ± 12.86 | 34.93 ± 13.43 | 36.43 ± 8.50 | 34.62 ± 8.81 | 0.008 | 0.002 | 0.074 |
| **IL eye** | **$D_{2\%}$ (Gy)** | 46.75 ± 6.30 | 46.89 ± 5.54 | 46.48 ± 5.15 | 45.55 ± 5.48 | 0.433 | 0.022 | 0.510 |
| **Spinal cord** | **$D_{2\%}$ (Gy)** | 15.08 ± 5.36 | 15.56 ± 5.57 | 9.13 ± 6.11 | 10.29 ± 6.91 | 0.001 | 0.001 | 0.001 |
| **Brainstem** | **$D_{2\%}$ (Gy)** | 37.96 ± 4.88 | 38.23 ± 4.68 | 28.10 ± 8.89 | 29.58 ± 8.21 | 0.045 | 0.013 | 0.002 |
| **CL temporal lobe** | **$D_{2\%}$ (Gy)** | 37.84 ± 10.57 | 37.78 ± 9.30 | 38.64 ± 7.95 | 38.94 ± 8.08 | 0.158 | 0.433 | 0.594 |
| **IL temporal lobe** | **$D_{2\%}$ (Gy)** | 49.76 ± 6.61 | 50.43 ± 6.17 | 45.61 ± 7.12 | 46.07 ± 6.82 | 0.510 | 0.397 | 0.003 |
| **CL cochlea** | **$D_{5\%}$ (Gy)** | 24.15 ± 13.68 | 24.53 ± 14.13 | 28.05 ± 8.55 | 28.52 ± 8.35 | 0.221 | 0.510 | 0.177 |
| | **$D_{mean}$ (Gy)** | 18.93 ± 10.81 | 19.05 ± 10.73 | 25.22 ± 6.99 | 25.53 ± 6.60 | 0.245 | 0.594 | 0.019 |
| **IL cochlea** | **$D_{5\%}$ (Gy)** | 33.32 ± 7.84 | 33.89 ± 8.33 | 31.34 ±7.61 | 33.57 ± 7.97 | 0.638 | 0.048 | 0.140 |
| | **$D_{mean}$ (Gy)** | 27.78 ± 6.63 | 27.75 ± 6.93 | 27.35 ± 5.42 | 29.57 ± 6.11 | 0.875 | 0.030 | 0.594 |
| **Pituitary** | **$D_{2\%}$ (Gy)** | 44.06 ± 9.41 | 44.41 ± 9.02 | 40.16 ± 12.54 | 41.45 ± 11.74 | 0.084 | 0.074 | 0.026 |
| **Oral cavity** | **$D_{50\%}$ (Gy)** | 16.83 ± 6.77 | 16.67 ± 6.67 | 8.11 ± 8.75 | 8.41 ± 8.38 | 0.245 | 0.026 | 0.002 |
| | **$D_{mean}$ (Gy)** | 22.27 ± 5.76 | 22.29 ± 5.78 | 16.73 ± 6.38 | 16.98 ± 6.21 | 0.594 | 0.022 | 0.002 |
| **CL parotid** | **$D_{50\%}$ (Gy)** | 5.03 ± 6.53 | 5.05 ± 6.39 | 7.14 ± 7.67 | 7.06 ± 6.97 | 0.109 | 0.315 | 0.003 |
| | **$D_{mean}$ (Gy)** | 6.02 ± 5.13 | 6.07 ± 5.05 | 8.94 ± 5.91 | 8.81 ± 5.38 | 0.060 | 0.975 | 0.002 |
| **IL parotid** | **$D_{50\%}$ (Gy)** | 7.98 ± 6.12 | 8.04 ± 6.10 | 8.69 ± 7.02 | 8.97 ± 7.02 | 0.233 | 0.069 | 0.875 |
| | **$D_{mean}$ (Gy)** | 9.03 ± 5.72 | 9.07 ± 5.68 | 10.90 ± 6.22 | 11.03 ± 6.22 | 0.300 | 0.551 | 0.004 |
| **Normal tissue** | **$V_{5Gy}$ (%)** | 39.2 ± 10.9 | 40.7 ± 11.4 | 31.8 ± 10.1 | 32.4 ± 10.4 | 0.001 | 0.001 | 0.001 |
| | **$V_{10Gy}$ (%)** | 22.3 ± 6.9 | 22.9 ± 7.1 | 23.5 ± 7.1 | 24.8 ± 7.6 | 0.001 | 0.001 | 0.054 |
| | **$V_{20Gy}$ (%)** | 10.7 ± 3.2 | 10.9 ± 3.3 | 11.9 ± 3.3 | 12.2 ± 3.4 | 0.002 | 0.009 | 0.002 |
| | **$V_{30Gy}$ (%)** | 5.6 ± 1.8 | 5.8 ± 1.8 | 6.4 ± 1.7 | 6.3 ± 1.7 | 0.006 | 0.085 | 0.001 |

PTV = planning target volume; CL = contalateral; IL = ipsilateral; $D_{x\%}$ = dose which is reached or exceeded in x% of the volume; $V_{xGy}$ = volume receiving at least x-Gy dose; HI = homogeneity index; CI = conformity index; $D_{mean}$ = mean dose.

doi:10.1371/journal.pone.0146604.t002

## MUs and delivery time

From the data presented in Table 3, increased number of MUs was observed for the use of FFF beams compared with conventional flattened beams, on average by 34.9% for IMRT and by 4.5% for VMAT. For IMRT, the FFF beams resulted in a decrease of beam-on time by an average of 42.2%, but the shorter beam-on time only translated into a reduction in the total treatment time by an average of 9.5%. For VMAT, no significant differences were found in terms of beam-on time and treatment time. Moreover, FFF-VMAT showed significant reductions of the MUs (by 66.3%) and treatment time (by 60.7%) compared to FFF-IMRT, although the pure beam-on time of FFF-IMRT was 55.0% less than that of FFF-VMAT.

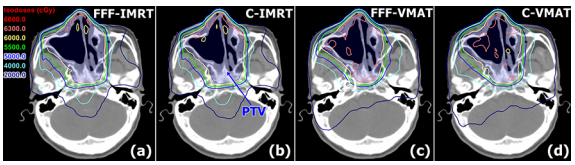


**Fig 1. Dose distributions of the flattening filter-free intensity-modulated radiotherapy (FFF-IMRT), conventional IMRT (C-IMRT), flattening filter-free volumetric modulated arc therapy (FFF-VMAT) and conventional VMAT (C-VMAT) plans for Patient 4.**

doi:10.1371/journal.pone.0146604.g001

## Discussion

As earlier published studies [6,8] have demonstrated, no significant dosimetric differences were observed between non-coplanar VMAT and coplanar VMAT for SNC, thus we only investigated the coplanar VMAT in this study for its advantage of less positioning uncertainty. In general, our data have implied that the FFF beams may provide encouraging results for the IMRT of SNC and comparable overall results for VMAT. For IMRT, the FFF beams reduced the doses to the contralateral lens, contralateral eye, spinal cord, brainstem and normal tissue, and improved the treatment efficiency. For VMAT, the FFF beams decreased the doses to spinal cord and several other OARs, but also increased the doses to the ipsilateral optic nerve and bilateral eyes, and maintained equivalent treatment efficiency. When the comparison of FFF-IMRT and FFF-VMAT is considered, FFF-IMRT obtained superior homogeneity and better sparing of contralateral optic structures and parotids, whereas FFF-VMAT had superior conformity and better sparing of several other structures.

Our finding that target dose coverage, conformity and homogeneity were comparable between FFF beams and conventional flattened beams in both IMRT and VMAT is similar to numerous other studies [17–19,22,23]. In modern radiotherapy techniques, the non-uniform dose distribution from a single open field of FFF beams can be compensated for by the increasing number of MUs which deposit dose at certain distances from beam's central axis where FFF fields deliver less dose per MU than flattened fields owing to the conical profile [17,18,20,23]. In addition, as the minimum dose of tumor predominately correlates with the tumor control probability (TCP) [28], the higher near-minimum dose to PTV_in_skin with FFF beams may have a positive impact on the TCP for the cases with superficial PTV. The relatively higher superficial dose is caused by the softened beam quality of FFF beams with elimination of the hardening effect of flattening filter. The percentage depth dose (PDD) distribution of 6-MV energy FFF beams was previously found to be close to that of conventional flattened 4-MV energy beams by Vassiliev *et al*'s study [13]. With regard to VMAT, though the anterior

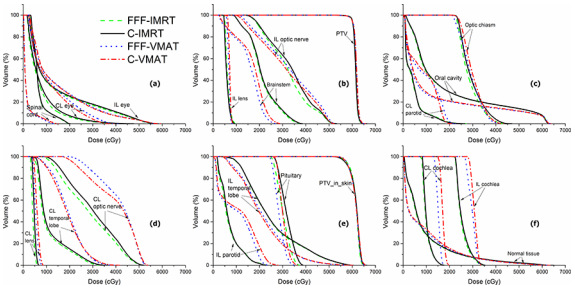


**Fig 2. Dose-volume histograms (DVHs) of the flattening filter-free intensity-modulated radiotherapy (FFF-IMRT), conventional IMRT (C-IMRT), flattening filter-free volumetric modulated arc therapy (FFF-VMAT) and conventional VMAT (C-VMAT) plans for Patient 4.**

doi:10.1371/journal.pone.0146604.g002

**Table 3. Delivery parameters for the conventional intensity-modulated radiotherapy (C-IMRT), flattening filter-free IMRT (FFF-IMRT), conventional volumetric modulated arc therapy (C-VMAT) and flattening filter-free VMAT (FFF-VMAT) plans.**

| | FFF-IMRT | C-IMRT | FFF-VMAT | C-VMAT | *P*-value | | |
|---|---|---|---|---|---|---|---|
| | | | | | FFF-IMRT *vs* C-IMRT | FFF-VMAT *vs* C-VMAT | FFF-IMRT *vs* FFF-VMAT |
| **Monitor units** | 1294 ± 172 | 964 ± 154 | 427 ± 23 | 409 ± 19 | 0.001 | 0.001 | 0.001 |
| **Treatment time (minute)** | 6.4 ± 0.2 | 7.0 ± 0.3 | 2.5 ± 0.0 | 2.5 ± 0.0 | 0.001 | 0.428 | 0.001 |
| **Beam-on time (minute)** | 0.9 ± 0.1 | 1.6 ± 0.3 | 2.1 ± 0.0 | 2.1 ± 0.0 | 0.001 | 0.066 | 0.001 |

doi:10.1371/journal.pone.0146604.t003

gantry angles could deliver a higher dose to PTV_in_skin, but the lower dose delivered to PTV_in_skin by posterior gantry angles counteracted this effect, resulting in similar doses between FFF-VMAT and C-VMAT. Moreover, our results showed that FFF-IMRT provided better dose uniformity than FFF-VMAT did, which is different from the results of other researches [4,6,7]. The explanation is that we used the special optimization approach mentioned above to improve our IMRT plan qualities [24]. This approach utilized the dose of the initial IMRT plan as a base dose for further optimization to compensate for the systematic optimization-convergence error [29], and as a result, the hot and cold spots were substantially reduced and the homogeneous dose distribution was achieved.

Our finding that the involvement of the contralateral lens and contralateral eye was significantly reduced by FFF-IMRT confirmed our conjecture and is in accordance with the characteristic of lower out-of-field dose. To our knowledge, none of the previous studies [17,19,21–23] has reported the sparing effect of FFF beams for IMRT, which may bring some potential clinical benefits to patients. The sparing of the optic pathway is crucial for the quality of life of the patients with long-term survival. Though Duprez *et al* [9] have concluded that the IMRT technique could minimize the ocular toxicity compared with conventional radiotherapy techniques, there were still 10 cases of late Grade 3 tearing and 1 case of late Grade 3 visual impairment in their group of 86 patients available for late toxicity evaluation. Similar studies were also presented in the review by Chi *et al* [10]. Furthermore, Ainsbury *et al* [30] suggested that radiation cataractogenesis may in fact be more accurately described by a linear, no-threshold model. Therefore, further reductions of doses to the optic structures are essential to obtain an optimal clinical outcome. On the other hand, FFF-VMAT showed inferior sparing of optic structures compared with FFF-IMRT and this may be attributed to the beam arrangement and fixed jaw technique aiming at minimizing the exposure to the lenses and other optic structures.

For both IMRT and VMAT, the FFF beams could reduce the doses deposited in the spinal cord and brainstem, which was expected to reduce the risks of radiation-induced myelitis and brainstem necrosis [31]. It could be beneficial to patients with locally residual or recurrent diseases, especially with a requirement of re-irradiation [32].

Our finding that the FFF beams reduced the $V_{5Gy}$, $V_{10Gy}$, $V_{20Gy}$, $V_{30Gy}$ to normal tissue by up to 1.4% is in favor of the research result presented by Nicolini *et al* [19], which found that FFF-VMAT reduced the $V_{10Gy}$ of healthy tissue by approximately 0.8% compared with C-VMAT. This is because the FFF beams could reduce collimator scatter and head leakage and consequently reduced the out-of-field dose [15,33]. Since the secondary cancer risk is closely associated with the exposure of normal tissue and total body [34], the FFF beams' efficacy of delivering lower dose to normal tissue and less head leakage may have a potential benefit of reducing the risk of secondary cancer, especially for young patients. However, a mitigating factor to this is the increased number of MUs of FFF plans, which would increase the tissue scatter from the treatment region.

Our result that the FFF beams obtained 9.5% reduction of treatment time and 42.2% reduction of beam-on time for IMRT is similar to Spruijt *et al*'s research [17]. They reported the 10% reduction of total treatment time and 31% reduction of beam-on time. Although the effect of the shortened treatment time is limited, FFF-IMRT would be more patient friendly and entail less likelihood of intrafraction shifts of tumor position. However, it is noteworthy that a few seconds of treatment time saved by the FFF beams can be thwarted because of a difference in patient setup time. When considering the VMAT technique, the treatment time required only 2.5 minutes in both FFF-VMAT and C-VMAT. The explanations of equal treatment/beam-on time for FFF-VMAT and C-VMAT were that the actual dose rates in both were around 200 MUs/minute, which were much lower than the maximum dose rates of 1400 and 600 MUs/minute selected, and the restricting factor of the treatment time was the gantry rotation, which already maintained a maximum speed of 6°/s during the dose delivery process.

To the best of our knowledge, our study is the first to report the impacts of FFF beams on the case of SNC. However, this is only a dosimetric study and a further study may be required to explore the clinical outcomes among these different techniques.

## Conclusion

For SNC treatment, the FFF beams yielded comparable target dose conformity, homogeneity, reduced normal-tissue doses and increased number of MUs compared with flattened beams in both IMRT and VMAT. The FFF beams demonstrated some improvements in contralateral optic structures and other structures as well as delivery efficiency in IMRT, whereas they provided comparable overall OAR sparing and delivery efficiency in VMAT. Our results suggest that using FFF beams in IMRT and VMAT is feasible for the treatment of SNC, and the delivery mode of FFF beams may play an encouraging role in IMRT, but yield comparable results in VMAT.

## Author Contributions

Conceived and designed the experiments: JYL BTH. Performed the experiments: JYL. Analyzed the data: JYL JZ. Contributed reagents/materials/analysis tools: JYL JZ WZZ. Wrote the paper: JYL JZ BTH. Revised the paper: WZZ.

## References

1. Mahalingappa YB, Khalil HS. Sinonasal malignancy: presentation and outcomes. J Laryngol Otol. 2014; 128: 654–657. doi: 10.1017/S0022215114001066 PMID: 25075949
2. Le QT, Fu KK, Kaplan M, Terris DJ, Fee WE, Goffinet DR. Treatment of maxillary sinus carcinoma: a comparison of the 1997 and 1977 American Joint Committee on cancer staging systems. Cancer. 1999; 86: 1700–1711. PMID: 10547542
3. Tiwari R, Hardillo JA, Mehta D, Slotman B, Tobi H, Croonenburg E, et al. Squamous cell carcinoma of maxillary sinus. Head Neck. 2000; 22: 164–169. PMID: 10679904
4. Jeong Y, Lee SW, Kwak J, Cho I, Yoon SM, Kim JH, et al. A dosimetric comparison of volumetric modulated arc therapy (VMAT) and non-coplanar intensity modulated radiotherapy (IMRT) for nasal cavity and paranasal sinus cancer. Radiat Oncol. 2014; 9: 193. doi: 10.1186/1748-717X-9-193 PMID: 25175383
5. Mock U, Georg D, Bogner J, Auberger T, Potter R. Treatment planning comparison of conventional, 3D conformal, and intensity-modulated photon (IMRT) and proton therapy for paranasal sinus carcinoma. Int J Radiat Oncol Biol Phys. 2004; 58: 147–154. PMID: 14697432
6. Orlandi E, Giandini T, Iannacone E, De Ponti E, Carrara M, Mongioj V, et al. Radiotherapy for unresectable sinonasal cancers: dosimetric comparison of intensity modulated radiation therapy with coplanar and non-coplanar volumetric modulated arc therapy. Radiother Oncol. 2014; 113: 260–266. doi: 10.1016/j.radonc.2014.11.024 PMID: 25467003

7. Nguyen K, Cummings D, Lanza VC, Morris K, Wang C, Sutton J, et al. A dosimetric comparative study: volumetric modulated arc therapy vs intensity-modulated radiation therapy in the treatment of nasal cavity carcinomas. Med Dosim. 2013; 38: 225–232. doi: 10.1016/j.meddos.2013.01.006 PMID: 23578496
8. Zhong-Hua N, Jing-Ting J, Xiao-Dong L, Jin-Ming M, Jun-Chong M, Jian-Xue J, et al. Coplanar VMAT vs. noncoplanar VMAT in the treatment of sinonasal cancer. Strahlenther Onkol. 2015; 191: 34–42. doi: 10.1007/s00066-014-0760-8 PMID: 25293728
9. Duprez F, Madani I, Morbee L, Bonte K, Deron P, Domjan V, et al. IMRT for sinonasal tumors minimizes severe late ocular toxicity and preserves disease control and survival. Int J Radiat Oncol Biol Phys. 2012; 83: 252–259. doi: 10.1016/j.ijrobp.2011.06.1977 PMID: 22027259
10. Chi A, Nguyen NP, Tse W, Sobremonte G, Concannon P, Zhu A. Intensity modulated radiotherapy for sinonasal malignancies with a focus on optic pathway preservation. J Hematol Oncol. 2013; 6: 4. doi: 10.1186/1756-8722-6-4 PMID: 23294673
11. Hoppe BS, Stegman LD, Zelefsky MJ, Rosenzweig KE, Wolden SL, Patel SG, et al. Treatment of nasal cavity and paranasal sinus cancer with modern radiotherapy techniques in the postoperative setting—the MSKCC experience. Int J Radiat Oncol Biol Phys. 2007; 67: 691–702. PMID: 17161557
12. Sheng K, Molloy JA, Larner JM, Read PW. A dosimetric comparison of non-coplanar IMRT versus Helical Tomotherapy for nasal cavity and paranasal sinus cancer. Radiother Oncol. 2007; 82: 174–178. PMID: 17275112
13. Vassiliev ON, Titt U, Ponisch F, Kry SF, Mohan R, Gillin MT. Dosimetric properties of photon beams from a flattening filter free clinical accelerator. Phys Med Biol. 2006; 51: 1907–1917. PMID: 16552113
14. Cashmore J. The characterization of unflattened photon beams from a 6 MV linear accelerator. Phys Med Biol. 2008; 53: 1933–1946. doi: 10.1088/0031-9155/53/7/009 PMID: 18364548
15. Kry SF, Vassiliev ON, Mohan R. Out-of-field photon dose following removal of the flattening filter from a medical accelerator. Phys Med Biol. 2010; 55: 2155–2166. doi: 10.1088/0031-9155/55/8/003 PMID: 20305334
16. Kragl G, Albrich D, Georg D. Radiation therapy with unflattened photon beams: dosimetric accuracy of advanced dose calculation algorithms. Radiother Oncol. 2011; 100: 417–423. doi: 10.1016/j.radonc.2011.09.001 PMID: 21945857
17. Spruijt KH, Dahele M, Cuijpers JP, Jeulink M, Rietveld D, Slotman BJ, et al. Flattening filter free vs flattened beams for breast irradiation. Int J Radiat Oncol Biol Phys. 2013; 85: 506–513. doi: 10.1016/j.ijrobp.2012.03.040 PMID: 22672750
18. Hrbacek J, Lang S, Graydon SN, Klock S, Riesterer O. Dosimetric comparison of flattened and unflattened beams for stereotactic ablative radiotherapy of stage I non-small cell lung cancer. Med Phys. 2014; 41: 031709. doi: 10.1118/1.4866231 PMID: 24593713
19. Nicolini G, Ghosh-Laskar S, Shrivastava SK, Banerjee S, Chaudhary S, Agarwal JP, et al. Volumetric modulation arc radiotherapy with flattening filter-free beams compared with static gantry IMRT and 3D conformal radiotherapy for advanced esophageal cancer: a feasibility study. Int J Radiat Oncol Biol Phys. 2012; 84: 553–560. doi: 10.1016/j.ijrobp.2011.12.041 PMID: 22386376
20. Zhuang M, Zhang T, Chen Z, Lin Z, Li D, Peng X, et al. Advanced nasopharyngeal carcinoma radiotherapy with volumetric modulated arcs and the potential role of flattening filter-free beams. Radiat Oncol. 2013; 8: 120. doi: 10.1186/1748-717X-8-120 PMID: 23672519
21. Dzierma Y, Nuesken FG, Fleckenstein J, Melchior P, Licht NP, Rube C. Comparative planning of flattening-filter-free and flat beam IMRT for hypopharynx cancer as a function of beam and segment number. PLoS One. 2014; 9: e94371. doi: 10.1371/journal.pone.0094371 PMID: 24722621
22. Gasic D, Ohlhues L, Brodin NP, Fog LS, Pommer T, Bangsgaard JP, et al. A treatment planning and delivery comparison of volumetric modulated arc therapy with or without flattening filter for gliomas, brain metastases, prostate, head/neck and early stage lung cancer. Acta Oncol. 2014; 53: 1005–1011. doi: 10.3109/0284186X.2014.925578 PMID: 24937551
23. Zwahlen DR, Lang S, Hrbacek J, Glanzmann C, Kloeck S, Najafi Y, et al. The use of photon beams of a flattening filter-free linear accelerator for hypofractionated volumetric modulated arc therapy in localized prostate cancer. Int J Radiat Oncol Biol Phys. 2012; 83: 1655–1660. doi: 10.1016/j.ijrobp.2011.10.019 PMID: 22572080
24. Lu JY, Wu LL, Zhang JY, Zheng J, Cheung ML, Ma CC, et al. Improving target dose coverage and organ-at-risk sparing in intensity-modulated radiotherapy of advanced laryngeal cancer by a simple optimization technique. Br J Radiol. 2015; 88: 20140654. doi: 10.1259/bjr.20140654 PMID: 25494885
25. Hodapp N. The ICRU Report 83: prescribing, recording and reporting photon-beam intensity-modulated radiation therapy (IMRT). Strahlenther Onkol. 2012; 188: 97–99. doi: 10.1007/s00066-011-0015-x PMID: 22234506

26. McGrath SD, Matuszak MM, Yan D, Kestin LL, Martinez AA, Grills IS. Volumetric modulated arc therapy for delivery of hypofractionated stereotactic lung radiotherapy: A dosimetric and treatment efficiency analysis. Radiother Oncol. 2010; 95: 153–157. doi: 10.1016/j.radonc.2009.12.039 PMID: 20116115

27. Paddick I. A simple scoring ratio to index the conformity of radiosurgical treatment plans. Technical note. J Neurosurg. 2000; 93: 219–222. PMID: 11143252

28. Gay HA, Niemierko A. A free program for calculating EUD-based NTCP and TCP in external beam radiotherapy. Phys Med. 2007; 23: 115–125. PMID: 17825595

29. Dogan N, Siebers JV, Keall PJ, Lerma F, Wu Y, Fatyga M, et al. Improving IMRT dose accuracy via deliverable Monte Carlo optimization for the treatment of head and neck cancer patients. Med Phys. 2006; 33: 4033–4043. PMID: 17153383

30. Ainsbury EA, Bouffler SD, Dorr W, Graw J, Muirhead CR, Edwards AA, et al. Radiation cataractogenesis: a review of recent studies. Radiat Res. 2009; 172: 1–9. doi: 10.1667/RR1688.1 PMID: 19580502

31. Siala W, Mnejja W, Khabir A, Ben Mahfoudh K, Boudawara T, Ghorbel A, et al. [Late neurotoxicity after nasopharyngeal carcinoma treatment]. Cancer Radiother. 2009; 13: 709–714. doi: 10.1016/j.canrad.2009.05.006 PMID: 19695928

32. Kan MW, Wong W, Leung LH, Yu PK, So RW, Cheng AC. A comprehensive dosimetric evaluation of using RapidArc volumetric-modulated arc therapy for the treatment of early-stage nasopharyngeal carcinoma. J Appl Clin Med Phys. 2012; 13: 3887. doi: 10.1120/jacmp.v13i6.3887 PMID: 23149781

33. Murray LJ, Thompson CM, Lilley J, Cosgrove V, Franks K, Sebag-Montefiore D, et al. Radiation-induced second primary cancer risks from modern external beam radiotherapy for early prostate cancer: impact of stereotactic ablative radiotherapy (SABR), volumetric modulated arc therapy (VMAT) and flattening filter free (FFF) radiotherapy. Phys Med Biol. 2015; 60: 1237–1257. doi: 10.1088/0031-9155/60/3/1237 PMID: 25590229

34. Hall EJ, Wuu CS. Radiation-induced second cancers: the impact of 3D-CRT and IMRT. Int J Radiat Oncol Biol Phys. 2003; 56: 83–88. PMID: 12694826